

2. ACCELERATOR AUGMENTATION PROGRAM

2.1 LINAC

S.Ghosh, A.Rai, P.Patra, G.K.Chowdhury, B.K.Sahu, A.Pandey, D.S.Mathuria, S.S.K.Sonti, K.K.Mistry, R.N. Dutt, J.Chacko, A.Chowdhury, S.Kar, S.Babu, M.Kumar, J.Antony, J.Zacharias, P.N.Prakash, T.S.Datta, A. Mandal, D.Kanjilal and A.Roy

2.1.1 Acceleration through all the eight resonators of linac cryostat # 1

To augment the energy of the ion beam from the Pelletron of Inter University Accelerator Centre (IUAC), a niobium based superconducting (SC) linac is under construction. Full linac will consist of five cryostats, the first one is the superbuncher cryostat housing single quarter wave resonator (QWR), the next three cryo-modules house eight QWRs each and the last cryostat has two QWRs to be used as re-buncher/de-buncher (Figure 1). At present, the SB cryostat, a single Linac module and the rebuncher (RB) are operational.

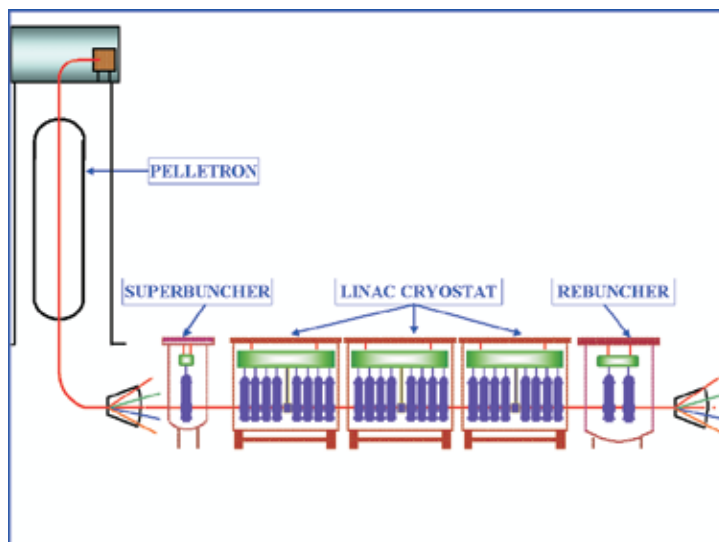


Fig. 1. The schematic of the Pelletron and Superconducting Linear accelerator of IUAC

In the past year the operation of LINAC was dedicated to conduct a number of scheduled experiments. During April-May 2009, for the first time at IUAC, all the eight LINAC resonators were operational and an average field (E_a) of ~ 4 MV/m were obtained from the eight QWRs (shown in figure 2). At the time of beam acceleration all the eight resonators of Linac#1 along with the resonators of SB and RB cryostats were locked against the master oscillator frequency of 97.000 MHz and all of them took part in the beam acceleration. During this period of a month, a variety of ion beams were accelerated and delivered for user

experiments [1]. Accelerated beam were used to conduct the Nuclear Physics and Material Science experiments in HYRA/Neutron line and Material Science beam line respectively. Table 1 lists the different beams, their energy gains (both from the Tandem and the LINAC) and their time widths at the entrance of the superbuncher, the LINAC and at the target location inside experimental chamber. Re-bunching with a time waist at the target was done in only three experiments though the resonators inside the rebuncher cryostat were made all the time ready. In the remaining four experiments, the rebuncher cavity was not operated as the time re-bunching was not required by the beam user.

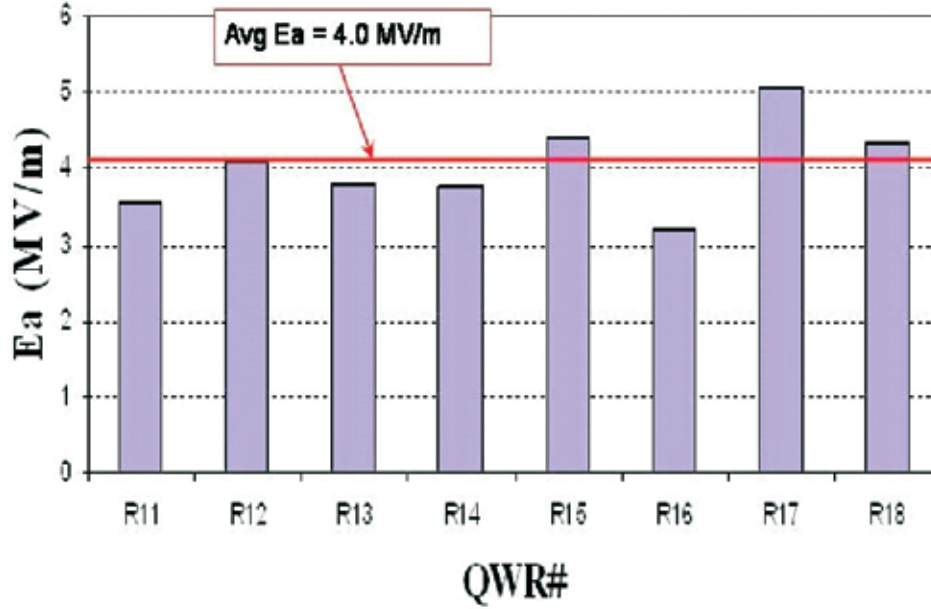


Fig. 2. The average accelerating fields from all the eight operational resonators of Linac#1.

Table 1: Parameters of the Ion Beams accelerated through LINAC

Beam	Energy from Tandem (MeV)	ΔT MHB (ns)	ΔT SB (ps)	Energy gain LINAC (MeV)	ΔT (RB) Target (ps)
$^{12}\text{C}^{+6}$	87	0.95	250	19.2	OFF
$^{16}\text{O}^{+8}$	100	0.95	163	18	342
$^{18}\text{O}^{+8}$	100	0.96	182	20	378
$^{19}\text{F}^{+9}$	115	1.08	190	25.8	354
$^{28}\text{Si}^{+11}$	130	1.2	182	37.5	OFF
$^{48}\text{Ti}^{+14}$	162	1.68	176	51.2	OFF
$^{107}\text{Ag}^{+21}$	225	1.7	232	74.6	OFF

2.1.2 Preparation of other resonators to be installed in linac cryostats 2 and 3

At present, the installation of the sixteen resonators in linac cryostats 2 and 3 is in progress. The indigenous resonators started to come out of fabrication from September '09. The final surface treatment, leak checking and cold performance tests on the resonators had been started since then. After a few initial low accelerating field measurements in a couple of resonators, finally higher electric fields of ~ 5 and 6.4 MV/m at 6 watts of input power in couple of resonators were achieved. Some more performance tests on the other resonators in test cryostat are necessary prior to the installation of the successful resonators in linac cryostats 2 and 3.

2.1.3 Use of Piezo-electric actuator as an alternative tuning mechanism of superconducting resonators

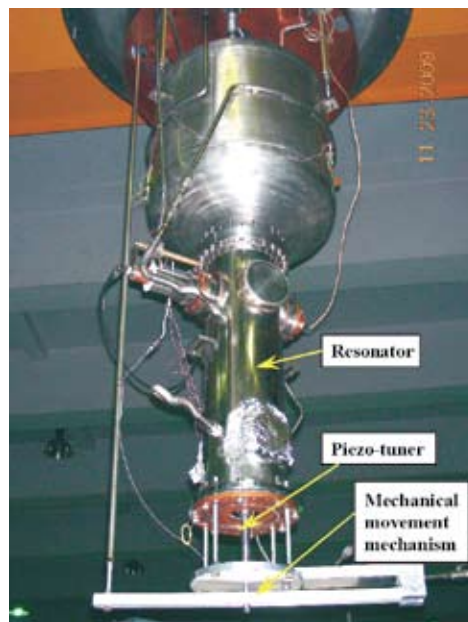


Fig. 1. The piezoelectric tuner along with a niobium resonator prior to its loading for a cold test in test cryostat

The present phase locking scheme of the resonators in the first operational module of the LINAC consists of a fast (electronic) and a slow (helium gas operated mechanical tuner) time scale control. In an alternate scheme to handle the slow time part of the phase control, the tuner plate is deflected by using a combination of a stepper motor for course adjustment and a Piezo electric crystal for fine adjustment of the frequency. The piezoelectric actuator is used for fine tuning of frequency and also used in closed loop along with dynamic I-Q based electronic tuner to phase lock the superconducting cavities. The piezoelectric tuner working in \sim milliseconds range has shared a substantial load from the electronic tuner. During a recent cold test of a QWR, the frequency range of the resonator in cold condition offered by

the Piezo was measured to be 1.6 KHz which corresponds to a total movement of $\sim 50 \mu\text{m}$ of the tuner plate. In this test, first the resonator was brought to 97.000 MHz (which is the operating frequency of the Linac) by the mechanical course tuner and then the resonator was locked at a field of 3.8 MV/m at 6 W of helium power and 40 W of amplifier power by the resonator controller with the Piezo electric tuner. With this successful test of the piezoelectric tuner, the new tuning mechanism will be used in all the resonators of linac cryostats 2 and 3, making the operation easier and more reliable.

REFERENCE

- [1] A. Rai et al, Proc. of 14th International conference on RF Superconductivity, September 17th to 19th 2009, Berlin, Germany, page – 244.

2.1.4 Superconducting Niobium Resonators

P.N.Prakash, K.K.Mistri, S.S.K.Sonti, A.Rai, J.Zacharias, S.Ghosh, P.Patra, G.K.Chowdhury, D.S.Mathuria, R.N.Dutt, A.Pandey, B.K.Sahu, D.Kanjilal & A.Roy

Production of a dozen niobium quarter wave resonators for the second and third linac modules is over. In cold tests at 4.5 K, the first two resonators tested so far, have exceeded the nominal design goal substantially. Work on the construction of two Single Spoke Resonators for Project-X of Fermi National Accelerator Laboratory (FNAL) has progressed well. Two Tesla-type Single Cell Cavities in niobium have been jointly built by IUAC and RRCAT, Indore. The first cold test on one of the Cavities at FNAL has indicated good performance.

2.1.4.1 Resonator Production for the 2nd & 3rd Linac Modules

The QWR production for the 2nd and 3rd linac modules aims to build fifteen niobium



Fig. 1. Bare niobium QWRs



Fig. 2. Slow Tuner Bellows assemblies

quarter wave resonators (QWRs). Out of this a dozen QWRs and all the fifteen Slow Tuner bellows have been completed. The remaining three resonators, which required reworking and had been kept aside, are also being completed now. In figure 1, the dozen production QWRs are shown. In figure 2, the niobium Slow Tuner bellows are shown.

The QWRs were tested at 4.5 K to check their performance. The initial results were not very encouraging. However, additional electropolishing to remove another 50 μm from the surface improved their performance substantially. In figure 3, the performance of the two resonators tested so far, is shown. QWR-I6, which was the first resonator to be tested, was cleaned in the ultrasonic cleaner using DI water at room temperature, after the final electropolishing and just before the cold test. QWR-I15, the next resonator to be tested, was also cleaned in the ultrasonic cleaner but with the DI water at $\sim 50^\circ\text{C}$. In addition, helium pulse processing at 5×10^{-5} mbar pressure was also performed on this resonator. Both the resonators were baked at $\sim 100^\circ\text{C}$ for at least 48 hrs. At low input powers (< 0.5 W) the accelerating electric fields produced in both the resonators are similar, indicating that the superconducting surfaces are more or less identical. The warm water ultrasonic cleaning has perhaps helped in achieving higher gradients in QWR-I15, as evident from the comparison at higher fields between the performances of the two resonators. The helium pulse processing further improved QWR-I15's high field performance (beyond 3.5 MV/m) by about 10%. In subsequent tests on other QWRs this recipe will be further investigated.

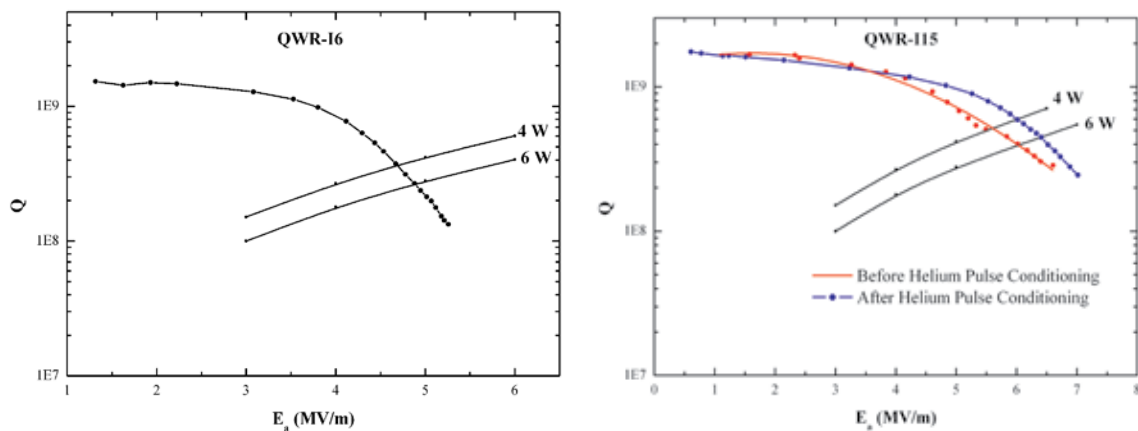


Fig. 3. Resonator Q as a function of the accelerating electric field E_a at 4.5 K for two resonators - QWR-I6 on the left, and QWR-I15 on the right.

2.1.4.2 Spoke Resonators

IUAC is currently building two Single Spoke Resonators ($\beta=0.22$, $f=325$ MHz) for Project-X at Fermi National Accelerator Laboratory (FNAL), USA. During the last one year substantial amount of development work was done on die forming the various niobium components. Figure 4a shows an Outer Shells setup for electron beam welding. Figure 4b

shows a Half Spoke formed in niobium. At present the Shells have been completed. The niobium Half Spokes have been formed and are being setup for e-beam welding. Forming of the End Wall will be taken up next. The brazed flange assemblies for the Beam Ports and Coupler Port pullouts have been received. We plan to complete the fabrication and ship the resonators to FNAL by August '2010.



Fig. 4. (a) Left, an Outer Shell setup for electron beam welding, and (b) Right, a Half Spoke formed in niobium.

2.1.4.3 Tesla-type Single Cell Cavity

As part of a joint collaborative project, Raja Ramanna Centre for Advanced Technology (RRCAT), Indore and IUAC have developed two Tesla-type Single Cell Cavities in niobium. This project had been initiated by RRCAT, which is planning a large program in this area, to start some initial activity in the field. In figure 5, one of the cavities is shown. Both the cavities have been sent to FNAL for further processing and testing. In cold test at 2 K the first cavity has produced 21 MV/m gradient limited by quench.



Fig. 5. Niobium Single Cell Tesla-type Cavity. The overall height is approximately 400 mm.

2.2 CRYOGENICS

T.S.Datta, J.Chacko, A .Choudhury, J. Antony, M. Kumar, S. Babu, S.Kar, D.S. Mathuria, R.N.Dutt, P. Konduru, A. Agnihotri, R.G. Sharma and A.Roy

In this academic year, the complete cryo-network system which includes liquid helium plant, cryogen distribution network and beam line cryomodules was operated successfully first time for more than a month at a stretch. The IInd and IIIrd Linac modules was developed and installed in the beam line after the preliminary test. The technical specification of the proposed new helium refrigerator along with process lay out to integrate with the existing system is finalized. Significant progress on superconducting magnet program is also reported here.

2.2.1 Cryogenic Facility

I. *Liquid Helium Plant*

The helium plant was operated twice for Linac operation six times for off-line testing of the resonators in simple test cryostat. The approximate running hour is 1133hrs and estimated total production of LHe was ~ 75000L.

Few major maintenance works has been initiated in this academic year. Cold engine was replaced but no significant improvement on cool-down time was noticed consistently. The vacuum of the inter connecting liquid helium line between the cold box and the 1000 L dewar is found to be deteriorated. The vacuum of the transfer line was improved by the prolonged baking and pumping. The improvement in vacuum in the transfer line reduces the cold down time of the plant from 24hrs. to 12 hrs. Oil leaking form the shaft seal of one of the compressor was arrested by complete overhauling.

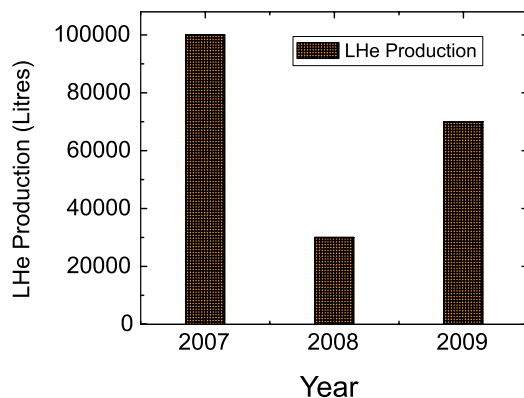


Fig. 1. Yearly Liquid Helium production.

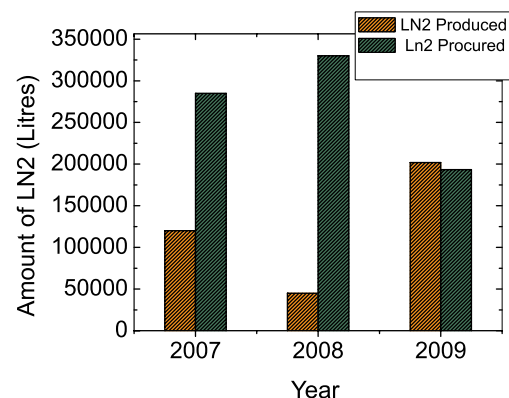


Fig. 2. Yearly Liquid Nitrogen production.

II. Liquid Nitrogen Plant

The plant was operated for 3867Hrs and estimated liquid nitrogen production was 1, 93,350 L. LN2 procured from outside vendor was 2, 01,941 L. The procurement of LN2 from outside vendor was reduced because of enhancement of capacity of in-house LN2 plant.

III. Liquid nitrogen Distribution Line

A new vacuum jacketed LN2 transfer line has been integrated with the external LN2 tanks to the existing LN2 network in Beam Hall II. Similar LN2 transfer line has also been integrated with the INGA LN2 dewar for INGA detector cooling. Total length of piping is about 125 meters in spools of 6 meters each with bayonet joints. The transfer line has been tested successfully. The filling time for the INGA LN2 dewar has been reduced substantially by using the new LN2 transfer line.

2.2.2 LINAC Cryomodules

I. Development of Linac Cryomodule II & III

In this academic year, the fabrication of the IInd and IIIrd Linac cryomodules have been completed. All the components like LHe vessel, LN2 vessel etc had undergone individual thermal cycling at LN2 temperature and each components were being helium leak tested prior to the integration in the cryomodules. The turbo pump of 2000LPS of pumping speed has been mounted in each cryomodule. For IInd cryomodules, the vacuum achieved at room temperature is 4E-6mbar. The vacuum improved to 9E-7mbar with LN2 in both LHe and LN2 Vessel. The vacuum achieved at room temperature for the IInd Linac module is 3E-6mbar. The typical pump-down profile of the IInd cryomodule is shown in Fig.3. The cryomodule was leak tested using MSLD.

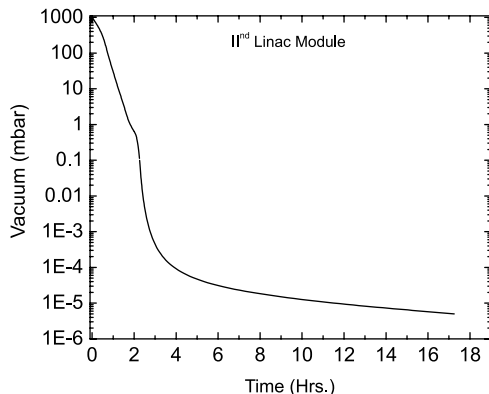


Fig. 3. Pump Down profile of Linac Cryomodule-II.



Fig. 4. The vacuum test of Linac Cryomodule -II

Both the cryomodules are installed in the beam line and their coarse alignment has been checked both at atmospheric condition and vacuum condition. The liquid helium cold test for both cryomodules is yet to be done. The Fig. 5 shows the IInd and IIIrd Linac cryomodules in the Linac beam line.



Fig. 5. The IInd and IIIrd Linac cryomodules in the Linac beam line

2.2.3 Other Development Projects

1. DST Project on Development of 6 Tesla Cryogen free Superconducting Magnet System (CFMS)

A 6 Tesla superconducting solenoid magnet, made of NbTi, has been designed and developed. The design parameters of the superconducting magnet are given in the Table 1. This 6 Tesla magnet will be conduction cooled by cryocooler, the wet-winding technique has been followed using room-temperature cured epoxy to enhance the layer to layer heat transfer. The winding of the superconducting magnet has been completed. The cold test and training of the magnet is yet to be done.

The design of the warm bore cryogen free magnet cryostat has been completed and the cryostat is under fabrication. The detailed thermal calculation has been done for the cryostat to match the limited refrigeration capacity of cryocooler.

Table 1: Parameters of the Superconducting magnet

Designed Magnetic field	6T @90A
S.C Material	NbTi
Wire Diameter	0.54mm
S.C: Cu	1:1.8
Internal Diameter of Winding	104 mm
Outer Diameter of Winding	136 mm
Winding length	200 mm
Total Number of Turns	200 mm
Total Number of Turns	10723
Total Number of Layers	30

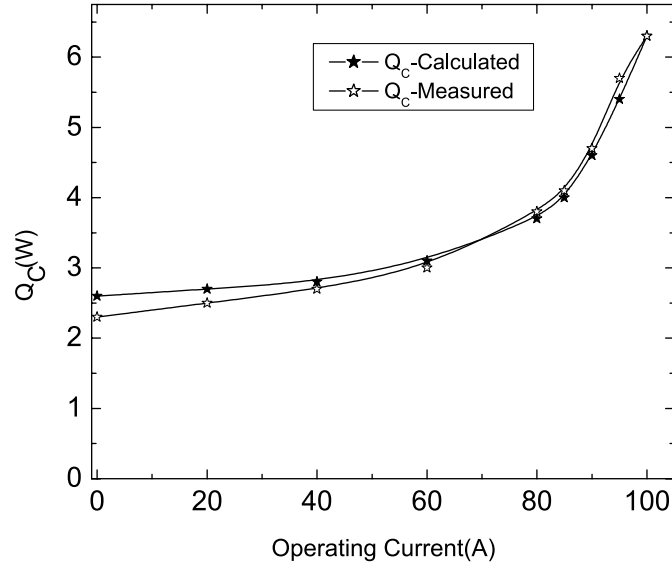


Fig. 6. The estimated and experimentally measured heat input to the 1st stage of cryocooler through the optimized copper current lead.

The key technology for development of a conduction-cooled superconducting magnet lies in reduction of heat inputs at both stages of cryocooler within its very limited heat budget at 4K. In any conventional superconducting magnet system, the main heat input comes from the copper current leads of the magnet. Based on the earlier experimental data reported last year, to reduce the heat input per ampere current, the current leads need to be optimized for current and dimension. The copper current lead, of RRR value 150, has been optimized numerically for temperature range 300K to 33K for 90A operating current. Experimental studies have been done on thermal and thermo-electrical behavior of the hybrid current lead for both optimized and non-optimized operation of the magnet and it has compared with a theoretical model

2. BRNS Project on Helium Purification through Membrane

A BRNS project was taken to study the feasibility of purification of helium gas from a mixture of helium and nitrogen. An experimental setup was developed with membrane modules, the analyzer, the flow elements and the gas manifold. Three different sets of membrane were procured from different suppliers (i) Medal helium separation membrane from AirLiquide, USA (obtained from VECC, Kolkata), (ii) helium separation membrane from UBE, USA (iii) Hiflux air separation membrane from Parker, USA. The third set of membrane, which is commonly used for separation of nitrogen and oxygen, was chosen to see the feasibility of separating the helium and nitrogen. A series of experiments were carried out with different concentration of gases in these membranes at different pressures and flow rates. The Table 2 summarizes the results of all three membranes.

Table. 2 The summary of the performances of different Membrane

Membrane Type	Air Liquide	UBE	Parker
Inlet Pressure (psig)	200-400	100	150
Inlet impurity (%)	31	30	29
Outlet purity (%)	92-95	84-92	52
Recovery ratio (%)	26-47	92	98
Recovery flow rate (NM3/hr)	0.06-0.168	0.372-0.996	3.48-5.12

3. Superconducting Quadrupole Magnet Program for HYRA

A superconducting quadrupole doublet is planned in place of a room temperature doublet quadrupole magnet as a part of HYbrid Recoil Mass Analyser (HYRA). For an independent operation of HYRA, magnet cryostat is based on helium reliquefaction concept based on using two stage 4.5 K cryocooler and hybrid current leads (HTS + Cu). The cryostat has been ordered and all the components have been fabricated and to test the assembly sequencing a mock up assembly was done at factory site (without the superconducting magnet). The development of the superconducting quadrupole coils is delayed because of the priority on development of LINAC Cryomodules.

A heat exchanger unit has been indigenously designed and tested for recondensation of evaporated helium gas in the quadrupole cryostat. Fig 7 shows the HX unit consisting of copper fins housed in SS chamber. The recondenser unit was tested independently and a LHe production rate of 44.6 cc/hr has been achieved and for the same unit the refrigeration capacity measured was 2258 miliwatt at 8.2 psi equilibrium chamber pressure (fig 8).



Fig 7. The heat exchanger block of recondenser

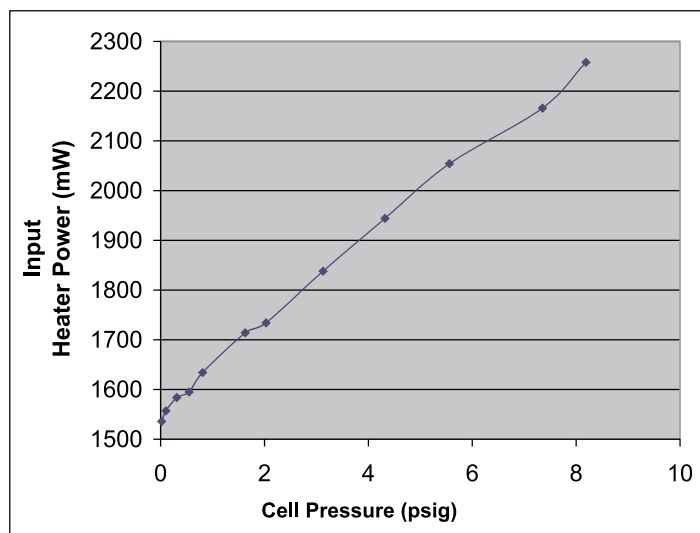


Fig. 8. The recondensation capacity at various input power in liquid helium against the stabilized chamber pressure.

4. Cryo-Instrumentation and Data Acquisition

VME based CRYO-DACS, which has been in operation since 2002, had two VME create failure issues this year. In both cases, the problem was pertained to M/s Elma make VME Crates and the Power supply unit has been found to be the component damaged. Necessary follow up is being made with the supplier as well as manufacturer to know the root cause of this failure, meanwhile the CRYO-DACS has brought to normal operation by replacing with spare crates.

CRYO-DACS up gradation plans are worked out to upgrade the present system which has some obsolete software and hardware. An Eight channel CAMAC programmable PPG (programmable Pulse generator) is being designed and tested to use with high power conditioning of superconducting resonators.

2.3 RF ELECTRONICS

A. Sarkar, S. Venkataramanan, B.K. Sahu, A. Pandey, and B.P. Ajith kumar

2.3.1 Status Report of the Multi-harmonic Buncher & the High Energy Sweeper and associated jobs

The multi-harmonic buncher (MHB) was operated along with the low energy chopper (LEC) to provide 4 MHz pulsed beams to several Linac users for the first time. Beams that were pulsed for the Linac operation included ^{12}C , ^{16}O , ^{28}Si , ^{48}Ti and ^{107}Ag . The FWHM of

the beam bunch varied from 0.8ns (for ^{12}C) to 2.3ns (for ^{107}Ag). The users were M.Zulfekar (JMI), Rohit Sandal (Punjab University), HYRA-Group (IUAC), Mat. Sc. Group (IUAC) and Linac-Group (IUAC). All the beam runs went quite smoothly without any major problem.

The system was also used to provide pulsed beams to several Pelletron users as well. The users were Sunil Kalkal (Delhi Univ.), Somen Chanda (Calcutta Univ.), K S Golda (IUAC), A.K. Bhatti (Punjab Univ.) . The beams that were pulsed included ^{12}C , ^{19}F , ^{14}N , ^{28}Si . The FWHM of the beam bunch varied from 0.8ns to 1.6ns. ^{14}N beam in Somen Chanda's run was the first pulsed beam to INGA.

2.4 BEAM TRANSPORT SYSTEM

A.Mandal, Rajesh Kumar, S.K.Suman, Mukesh Kumar and Sarvesh Kumar

Beam transport system laboratory takes care of regular maintenance, design and development of accelerator beam transport system with their beam optics simulations and field computation. This year the detailed beam optics for new low energy ion beam facility has been worked out. Beam optics for HCI is being simulated for various options. Different beam transport elements viz. magnetic and electrostatic quadrupoles, beam diagnostic elements etc are being developed for new LEIBF and HCI facilities. Power supplies for different magnets have been indigenously developed. Other than power supplies the group is actively involved in development of equipments for the others lab at IUAC. Details of development activities are summarised below.

2.4.1 Design of new Low Energy Ion Beam Facility

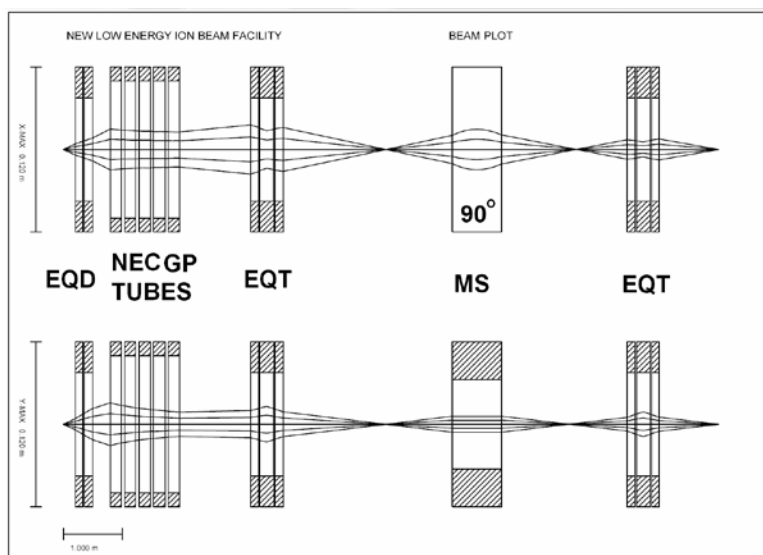


Fig. 1a. Beam optics of 900 beam line using GICOSY code

The beam optics of new low energy ion beam facility has been studied extensively by taking the realistic case of Ar ion beam with variable energy, emittance, space charge and also changing the structure of accelerating tube by TRANSPORT code. The similar calculation also repeated in GICOSY as shown in fig. 1a and tuning parameters obtained from both codes matches very closely. Finally whole layout is given in fig. 1b.

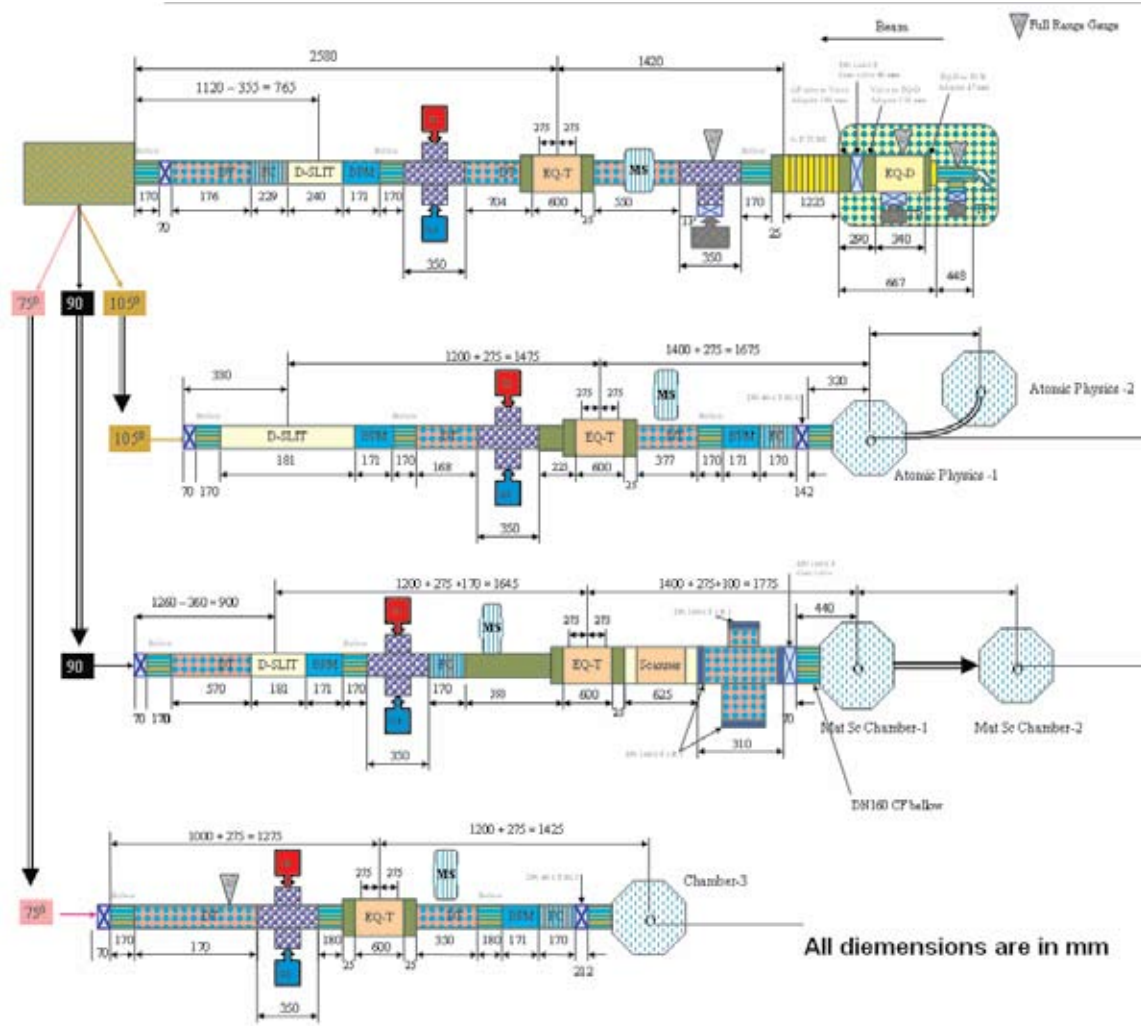


Fig. 1b. Layout of new LEIBF in Mat. Sc. Building (All dimensions are in mm)

2.4.2 Beam Optics of High Current Injector

The beam optics of high current injector is being divided into three different energy regime parts as follows:

- I. Low energy beam transport section (LEBT)
- II. RFQ to DTL matching section

III. Medium energy beam transport section (MEBT)

- a) Design-I
- b) Design-II

I. Low energy beam transport section (LEBT)

The beam optics of LEBT section has been studied in both manners transverse and longitudinal extensively by TRANSPORT, GICOSY and TRACE3D within first order. The input beam parameters of this section are given in table 1. A magnetic quadrupole doublet is being put up at the extraction of high temperature superconducting ECR ion source (HTS-ECRIS) and beam is analysed to select $A/q = 6$ by analyzing magnet. Then the beam is transported with the help of electrostatic quadrupole triplet, accelerating section and a set of four magnetic quadrupole to the RFQ entrance. The 12.125 MHz multi harmonic buncher is being placed at the waist formed after the accelerating section.

Table 1: Input beam parameters of LEBT

Emittance (ϵ_x and ϵ_y)	100π mm-mrad
Mass to charge ratio (A/q)	6
Max. magnetic rigidity (Bρ)	0.09 Tm
Initial energy (E)	30keV/q

II. RFQ to DTL section

The matching section extends from exit of RFQ to entrance of DTL. The radio frequency quadrupole provides the acceleration of ion beam coming from LEBT section with the energy of 8keV/u to the energy of 180keV/u. The initial ion beam parameters of this section are given in table 2.

Table 2: Ion beam parameters at the exit of RFQ

Emittance (ϵ_x and ϵ_y)	35π mm-mrad
Mass to charge ratio (A/q)	6
Max. magnetic rigidity (Bρ)	0.36Tm
Initial energy (E)	180keV/u

The accelerated beam is transported to DTL by a set of quadrupole magnets. The purpose of matching section is to match the beam into successive device in all phase space along with suitable space for beam diagnostics. The double gap 48.5 Mhz spiral buncher is used to provide appropriate phase matching to the entrance of DTL for the beam coming from RFQ. We have studied two designs which correspond to short and long matching section with a flexibility of optimum distance between RFQ to DTL. Both designs have their own advantages and disadvantages over each other. The detailed transverse and longitudinal beam optics of both designs have been done using the code TRACE 3D. Finally we approach to appropriate design with proper advantages of minimum quadrupole gradients required and minimum phase growth up to the spiral buncher simultaneously.

III. Medium energy beam transport section (MEBT)

The initial ion beam parameters are given in table 3. The medium energy beam transport section of high current injector accepts the beam from drift tube linac (DTL) and delivers it to entrance of superconducting LINAC. The DTL produces a beam of maximum energy of 1.8 MeV/u. The aim of MEBT design is to transport the beam to LINAC entrance without beam loss and emittance growth and to provide flexibility in the transverse and longitudinal beam spot size finally. The DTL produces beam with an energy spread of 1 to 1.5%. The bending of such beam at high energy (MeV) leads to dispersion and thus growth in transverse emittance. So we have decided to go for achromat bends in which dispersion due to one magnet gets cancelled by another magnet. The design parameters have been adjusted in order to give 1:1 object to image transport in beam size and according to geometry constraints. The edge angles of bending magnets involved in the achromat design are reduced to as lowest as possible. All the quadrupole gradients used for focusing the beam involved in MEBT section are less than 10T/m. Both transverse and longitudinal beam optics has been studied using code GICOSY, TRANSPORT and TRACE3D. The RF bunchers have been placed at the appropriate location to compenstate the phase growth. The two different MEBT designs-I and II options have been studied to transport the beam from beam hall-3 to beam hall-1.

Table 3: Ion beam parameters at the exit of DTL

Emittance (ϵ_x and ϵ_y)	9π mm-mrad
Mass to charge ratio (A/q)	6
Max. magnetic rigidity (Bρ)	1.15 Tm
Initial energy (E)	1.8 MeV/u

a) Design-I: The overall layout of HCI demands a total bending of 360 deg. so as to enter the beam into superconducting LINAC. To meet the design criteria, we have decided to design two achromat bends of 90 deg. and and one achromat bend of 180 deg. The beam optics work has also been verified by the multiparticle simulation code TRACK.

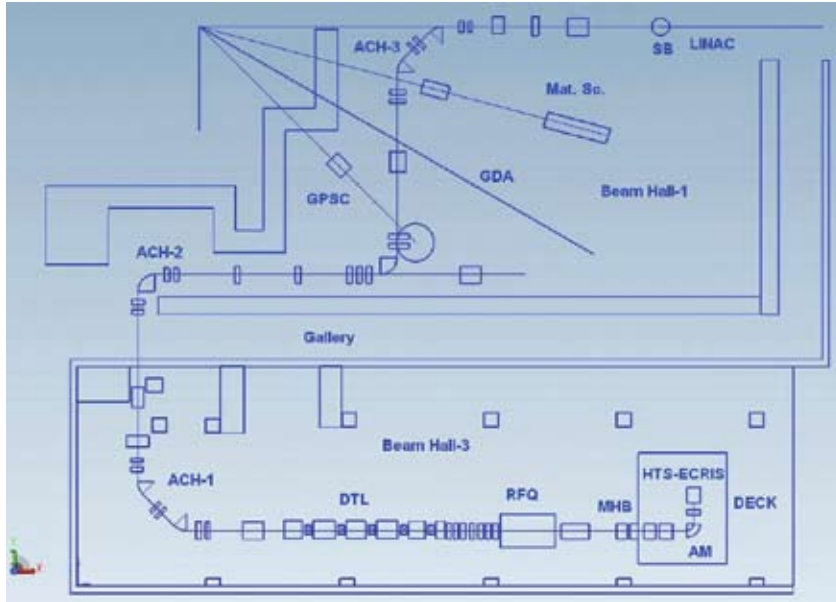


Fig. 2a. Layout of full MEBT section using TRACE3D code (Design-I)

b) **Design-II:** In this design, beam enters from beam hall-3 to beam hall-1 at an inclined angle of 114 deg and thus require a hole into the radiation safety wall (1m thickness) of beam hall-1. The design consists of two achromat bends of 114deg. and 66deg. However one more 66 deg. achromat bend is required in beam hall-1 to construct a new experimental beam line in future. The position of buncher after DTL depends on the energy spread coming out of DTL to compensate the phase growth.

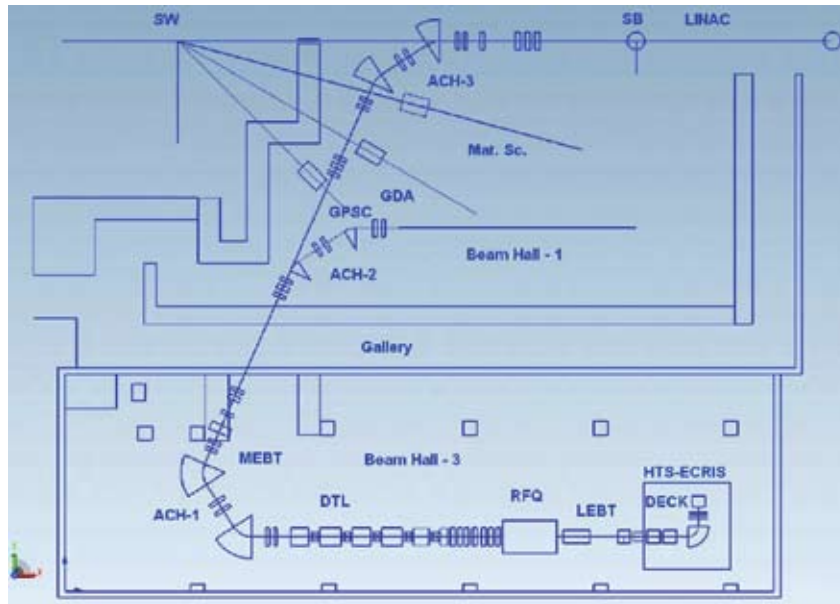


Fig. 2b. Layout of full MEBT section using TRACE3D code (Design-II)

Comparison of design-I and II of MEBT section:

We have compared the above two design in terms of hardware requirements and other geometrical parameters and the comparison is given in table 4. Both designs have their own advantages and disadvantages over each other. In design-II, the high voltage deck in LEBT section has to be shifted backward to avoid hitting the existing support structure pillar in MEBT section. Also the space for putting beam diagnostics containing stripper is very limited at the DTL exit. The alignment of beam lines is much simpler in design-I due to right angle bends.

Table 4: Comparison of two design options of MEBT

Design Parameters	Design-I 45-45, 90-90, 45-45	Design-II 57-57, 33-33, 33-33
Total length (m)	50	37.5
No. of achromatic bend	3	3
No. of quadrupoles triplet	6	3
No. of quadrupole singlet	22	13
No. of dipole magnet	6	6
Radiation safety wall breakage	No	Yes
No. of buncher required	2	2
Distance of first buncher from DTL (m)	9.2	7.5
Distance of second buncher from Superbuncher (m)	7.5	6.5

2.4.3 Design of 48.5 MHz RF bunchers for HCI

The 48.5 Mhz bunchers in RFQ to DTL matching section and MEBT section are spiral two rf gap cavity. Some designing parameters have been listed in table 5. The spiral bunchers are preferred due to their high shunt impedance, good mechanical strength and compact structure. However the design is being studied with different possible spiral structure by CST microwave studio for determining quality factor, shunt impedance etc.

Table 5: Designing parameters of HCI bunchers

Parameters	Buncher after RFQ in Archimedean spiral	Buncher after DTL in Archimedean spiral
Resonant Frequency	48.5MHz	48.5 MHz
Velocity (β)	0.0196	0.062
Operating Energy	0.180 MeV/u	1.8 MeV/u
Length of Cavity ($\beta\lambda$)	121.6 mm	383.4 mm
Spiral depth in beam direction	30 mm	50 mm
Spiral Width in x-y plane	40 mm	40 mm
Spiral Pitch	20mm	20mm
Arc Length of Spiral $\lambda/4$ (mm)	2078 mm	2078 mm

2.4.4 Power supplies ($\pm 10A/15V$) for magnetic micro steerers:

Two micro steerers are required in between two LINAC cryostates for fine tuning of the beam through LINAC. Four power supplies for these steerers have been assembled in house, tested and kept ready for installation. These are $\pm 10A/15V$ bipolar current regulated power supplies based on linear series pass technique. These are bipolar transconductance amplifier based on linear series pass technique with “class- AB” push pull output stage. The load current is sensed by the sensing resistor (shunt). Regulation is achieved by comparing the voltage drop across the shunt resistor with the control signal. The resultant error signal controls the output current through the bipolar output stage transistor bank such that the output current follows the control signal. Safety interlocks have been provided for safe operation. The power supply can be controlled locally through front panel and remotely through CAMAC IGOR interface. Large output capacitors are used to stabilize the loop to drive inductive loads.

2.4.5 Power supplies ($\pm 3A/30V$) for LEIBF steerer magnets:

Two magnetic Steerers are needed at new LEIBF facility. Four power supplies ($\pm 3A/30V$) have been assembled in house and tested. These linear DC current regulated power supplies use a fixed diode rectifier to convert mains AC to DC, and a series pass transistor stage to regulate the output. These power supplies can be controlled manually from front panel and remotely via CAMAC interface. To ensure, low ripple with short term and long term stability a double loop regulation topology has been implemented that uses transistor

bank as series pass element. In order to ensure the precise setting of the power supply current 16 bit DAC is used which gives an output setting resolution of 15ppm. The bipolar operation of these power supplies provides a smooth transition through zero, eliminating the need for current reversal contactors or relays. The power supply control electronics has been designed in modules for ease of maintenance. Options for Peltier based temperature compensation and DCCT feedback has been provided to have high stability.

2.4.6 High voltage power supply (3kV, 200mA) for saddle field atom source:

The development of (3kV, 200mA) DC high voltage power supply for Saddle field atom source is taken as a technology development under a mission project of DST. This power supply is different than normal HV power supplies in a way that it can sustain continuous arcing at the output. In order to make the design more versatile we have decided to make a unit of 1000W. The power supply has been designed in modular fashion such that any output voltage (within 2kV to 50kV) can be assembled with the same design without much modification. Circuit design, layout plan, wiring plan and cabinet designs has been finalized. PCB design is in progress.

2.4.7 Linear bipolar HV amplifier (± 2 kV) for electrostatic steerer/ sweeper:

This is a general purpose HV linear bipolar amplifier with a bandwidth from DC to 100Hz. It can be used with electrostatic devices in scanning, steering and sweeping of low energy ion beams at high frequencies to attain uniform implantation. This is a linear bipolar voltage amplifier based on series negative feed back technique. In output stage high voltage IGBTs are used in class AB amplifier configuration. The unit consists of three independent ± 2 kV linear bipolar AC amplifiers for X1, Y1 and Y2- axis. The Y2 amplifier can be used for dog-leg operations. The unit has been provided with both local and remote controls. The instrument has been designed in a 19" card frame assembly. Cabinet, layout plans, wiring plans, panel designs and soft copies of circuits are ready. The instrument is in physical shape. PCB designs are in progress.

2.5 LOW ENERGY ION BEAM FACILITY (LEIBF)

2.5.1 10 GHz Electron Cyclotron Resonance Ion Source (ECRIS) based Low Energy Ion Beam Facility (LEIBF)

P. Kumar, G. Rodrigues, U. K. Rao, Y. Mathur, Raj Kumar, S. K. Saini, P. Barua, A. Kothari, S. Rao, C. P. Safvan and D. Kanjilal

ECRIS based LEIBF [1] is operational since 2000 and its performance has been satisfactory in the academic year 2009-2010. In this year, low energy ion beams of

different charge states, in the range of a few KeV to a few MeV, were developed and delivered successfully for materials science, atomic and molecular physics experiments. This energy range is most suitable for material engineering and modifications. The production of highly charged positive ions, which is specialty of ECR ion sources, is utilized to study atomic and molecular physics via ion-atom collision processes. The nickel beam developed using volatile compounds (MIVOC) [2] methods was used to fabricate ZnO based dilute magnetic semiconductor (DMS). Room temperature ferromagnetism was observed in ZnO/Si thin films due to implantation of 200 keV Ni²⁺ ions with fluence (ions/cm²) values 6×10^{15} ions/cm², 8×10^{15} ions/cm² and 2×10^{16} ions/cm² respectively. These ion fluences are equivalent to Ni concentration of ~2% (A1), ~3% (A2) and ~7% (A3) in the films. Ferromagnetic property was obtained without any pre or post heat treatment and was confirmed by Alternating Gradient Magnetometry (AGM). Saturation magnetisation (M_s), remanence (M_r) and coercivity (H_c) values were different for three different fluences. M_s and M_r values were maximum in the film corresponding to the ion fluence of 8×10^{15} ions/cm² whereas H_c value was minimum for this ion fluence. The resistivity value as measured by vander Pauw was also minimum for this case. In all the three films, no extra crystalline phases (apart from ZnO) was observed within the detection limit of grazing angle x-ray diffraction (GAXRD) technique. Surface morphology of the films was studied by atomic force microscopy. The results were understood on the basis of an exchange interaction of the charge carriers generated due to thermal effects of ion implantation and the localized spins of Ni. This research work has been published in Journal of Physics (JAP) [3].

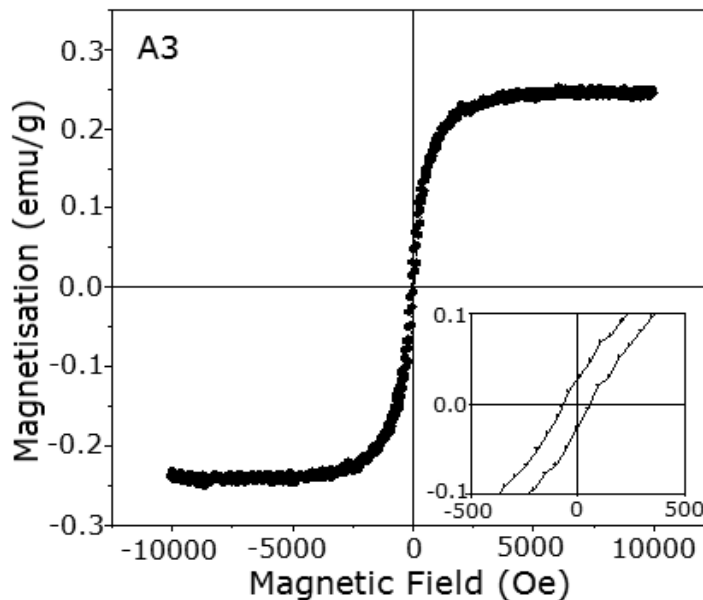


Fig.1. Alternating gradient magnetograph of thin film implanted with 7% Ni concentration

Thin films of ZnO prepared on sapphire substrates were also studied under same ion beam treatments and similar results were obtained. Further, thin film corresponding to 3% Ni concentration showed 80% transmittance across visible wavelength range. This report was also accepted recently for publication in JAP. There are reports where researchers have reported RT-FM in ZnO with out any doping of magnetic elements. Therefore, ZnO bulk samples were implanted with Ni and Ar ions. With Ar ions implantation, we produced the similar defects in ZnO to separate the defect mediated and carrier mediated ferromagnetsim. Furthermore, effect of thermal and athermal (Pelletron ion beam) annealing on RTF in ZnO was also planned.

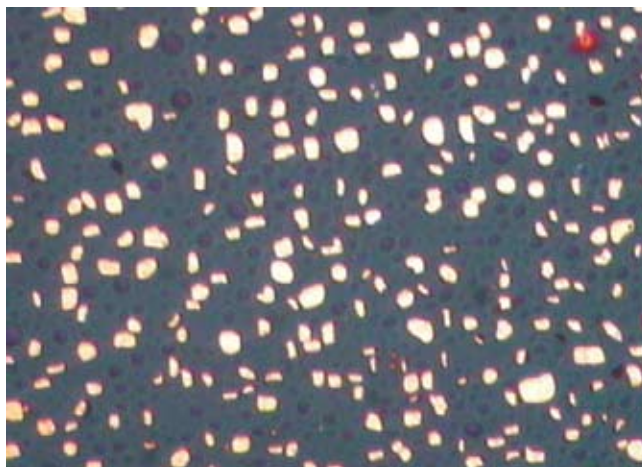


Fig. 2. Optical images of H⁺ implanted Ge surface (100 μm x 100 μm) at LN2 temperature. Post-implantation annealing was done at 500°C/0.5hr.

The light ions (H and He) implantation was mainly done for defects engineering of materials, specially semiconductors like Si, AlN, GaN and InP in collaboration with IIT Delhi group. The objective of this work is mainly to optimize the ion fluence for the formation of nano/microcracks in implanted semiconductors. Further, implantation parameters (ion current, ion energy, processing temperature) were optimized to get the controlled blistering in these semiconductors. Such studies are very useful to understand smart cut process by which semiconductors on insulators are synthesized now a days [4]. Two papers on this work were published in Phys. Status Solidi A and B. This work was awarded by first prize in National Conference on Advanced Materials and Radiation Physics (AMRP 2009), during 9-10 March 2009 at Sant Longowal Institute of Engineering and Technology, Sangrur, Punjab.

The experimental chamber equipped with time of flight and channeltron detectors to study the interaction of highly charged ion with molecules is up to date. Two students already completed their Ph.D using this apparatus and presently another student from Kolkatta university is perusing her Ph.D using the same setup.

Apart from collaborative research work, research proposals are invited from various universities/institutes to plan internationally competitive research programs. A two days

workshop on the use of low energy ions was conducted at IUAC during 9-10 July 2009. Out of total received research proposals, 27 were sanctioned for beam time. We successfully completed their beam time and only a few proposals are left.

The regular check of electronic and mechanical components installed in beam line and ion source resulted in minimal maintenance work during last academic year. Major maintenance works during last year were the repairing of traveling wave tube (TWT) amplifier, gas dosimetry valve controller and beam profile monitor (BPM) installed in post analysis section of LEIBF. The Rf window installed in injection side of the ion source got punctured during one of planned experiments. The new Rf window was installed and vacuum tests were completed.

The source and beam line pressures are low $\times 10^{-7}$ and high $\times 10^{-8}$ mbar respectively. The vacuum inside the experimental chamber is low $\times 10^{-7}$ mbar. The implantation chamber with facilities like target holders for mounting large number, implantation at different temperature conditions, PID temperature controller etc is up to date. In recent years, many imported equipments were repaired and in-house spare modules for the same were also developed. The low voltage power supply modules, high voltage filters, power factor conversion modules, high voltage diodes (all part of 200 W TWT amplifier) and PCB of gas dosimetry controller are few examples of that.

We are also in process of shifting the LEIBF in new building. For this, a double storey high voltage (400 kV) platform was designed and installed in the beam hall. A new DANFYSIK switching magnet with three exit ports has also been positioned. The high voltage testing (400 kV at 0.5 mA) of deck was completed. The ion optical design of new LEIBF was done using various simulation codes and finalized in position and dimension of various beam line components.

The LEIBF has been operational almost full time for delivery of various ion beams for regular experiments. The typical experiments, which were carried out include nanopatterning on different surfaces, light ion induced micro cracks in semiconductors – smart cut process for making semiconductors on Insulators (SOI), synthesis of Dilute Magnetic Semiconductors (DMS), controlled nanophase formation in various matrices, molecular dissociation by highly charged ions etc. Such experiments resulted in large number of publications in international referred journals. More than one dozen Ph.D scholars students completed their Ph.D using this facility. In this academic year, 4 LEIBF assisted research papers were selected for award in different national and international conferences. The facility is in regular operation and is being used by researchers/users from all over India and abroad.

REFERENCES

- [1] P. Kumar, G. Rodrigues, P. S. Lakshmy, D. Kanjilal, R. Kumar, J. Vac. Sci. Technol. A, 26(1), 97 (2008).

- [2] P. Kumar, G. Rogrigues, P. S. Lakshmy, D. Kanjilal, Beer Pal Singh, R. Kumar, Nucl. Instr. And Meth. B, 252 (2006) 354.
- [3] B. Pandey, S. Ghosh, P. Srivastava, P. Kumar, D. Kanjilal, J. Appl. Phys. 105, (2009) 033909.
- [4] R. Singh, I. Radu, U. Goesele, and S. H. Christiansen, Phys. Status Solidi C 3, (2006) 1754.

2.5.2 High Temperature Superconducting ECRIS -PKDELIS and Low Energy Beam Transport (LEBT)

G. Rodrigues, P. S. Lakshmy, Y.Mathur, U.K.Rao, R.Ahuja, R.N.Dutt, A.Mandal, D.Kanjilal and A.Roy

A. Source Operations



Fig. 1. A view of the 18 GHz HTS ECR, PKDELIS and associated LEBT

The state of the art ECR source PKDELIS has been in regular operation during the academic year 2009 and the low energy beam transport section was modified to install beam diagnostic system consisting of double slit and beam profile monitors. The aim was to mainly to measure the beam emittance from the source and to get an overall idea for proper matching of the optics for the downstream accelerators like RFQ and DTL. The details of the measurement are listed below. Additionally, the beam profile measurements could further confirm the simulated optics through the LEBT [3,5]. Heavier beams like krypton and xenon were tuned to maximize the beam currents of the higher charge states. Further work is going on to improve the beam intensities specially for beams with $A/q \sim 6$ which is the design goal for accelerating beams through the high current injector. Heavy ion beam development is in continuous progress. Model calculations predict that further improvements are possible to obtain higher intensities of highly charged ions.

The x-ray Bremsstrahlung measurements [6,4] performed as a function of negative dc bias voltage (by keeping the extraction voltage in the off condition) has shown that the high temperature component of the electrons is altered significantly using the dc bias voltage and the electron populations have to be maximized for extracting higher beam currents for the case of medium and highly charged ions of argon. Further work is going on to study the influence of other source parameters on the x-ray Bremsstrahlung.

In the last year we faced problem with the 1.7 kW, 18Ghz Klystron Power Generator. It was tripping frequently showing voltage overload. We diagnosed that it was due to dust in the high voltage section of the power generator. Its high voltage section was then cleaned properly. This solved the problem.

We encountered the problem of frequent tripping of the HTS coils which was most probably due to the 6V,200A Xantrex power supply of injection coil and the faulty PT-100 temperature sensor in the injection warm lead.. Since it was practically not feasible to change the sensor at that time, the signal from the sensor was temporarily disabled. This solved the problem only partially. After observing the tripping pattern more carefully it was analyzed that its injection power supply was not stable in the voltage mode of operation. So we replaced it with the spare 6V, 200A power supply and solved the problem. The old power supply is being looked into to solve the problem permanently.

Some up-gradation in the control system has been pursued especially for the oven control system of the PKDELIS source. It uses a typical light link for isolation and communicating to the 60 kV high voltage deck controls. This oven control has a wireless communication with the main control system of PKDELIS.

The monitor of cryostat coils temperature has also been added in the PKDELIS controls and is depicted in the graphical form in the cryostat page of control program. Also the remote reset of the xantrax power supplies for solenoid coils has been added.

B. Optics for the low energy beam transport (LEBT)

The optics from the source up to the post-analysed faraday cup has been looked into some detail. Extraction voltages around 15 kV to 20 kV have been found to be optimum for reasonable transmission and also for stable operation. However, higher extraction voltages beyond 20 kV causes over-focussing and the transmission through the system deteriorates. A beam viewer (quartz) just before the post-analyser faraday cup clearly shows that the beam is focussed (y-direction) at a position somewhere up-stream of the quartz which also roughly matches with the simulations. A GIOS simulation shows the profiles through the LEBT at an extraction voltage of 15 kV. The ion trajectories just after extraction at a typical extraction voltage of 30 kV is implemented in the newly designed extraction system. This system will be used for transporting the beam with additional voltage of 30 kV from the high voltage

platform to further inject into the RFQ and DTL accelerators. Further modifications are going on to improve the transmission through the LEBT.

C. 3D Modelling of the magnetic structure of 18 GHz HTS ECR PKDELIS

3D modelling of the magnetic structure of the 18 GHz HTS ECR, PKDELIS was initiated to understand the feasibility of two-frequency coupling. As a part of the improvement of the source performance, adding an additional frequency (two-frequency operation) has added benefits as observed from various ECR sources around the world. In order to explore the possibility, we have tried to simulate the ECR surfaces for various frequencies corresponding to operating magnetic fields. Frequencies lower than 18 GHz are always possible due to the magnetic field structure; however, higher frequencies are limited due to the maximum operating magnetic fields of 1.8 and 1.5 tesla for the injection and extraction sides respectively. The simulation shows the optimised ECR surfaces which correspond to typical operating currents of 120 A and 80 A on the injection and extraction coils for highly charged ions like Ar^{11+} etc. The minimum frequency that can allow us to operate is roughly 12.6 GHz corresponding to B_{ecr} of 0.45 T.

In order to check the validity of the model, the typical triangular pattern observed on the plasma electrode positioned at various locations have been checked with the models. Fairly good agreement has been observed. Figure 2 shows the observed triangular pattern on the plasma electrode together with the model. It is also expected that the model can help to improve the understanding of the confinement of the plasma and extraction conditions.

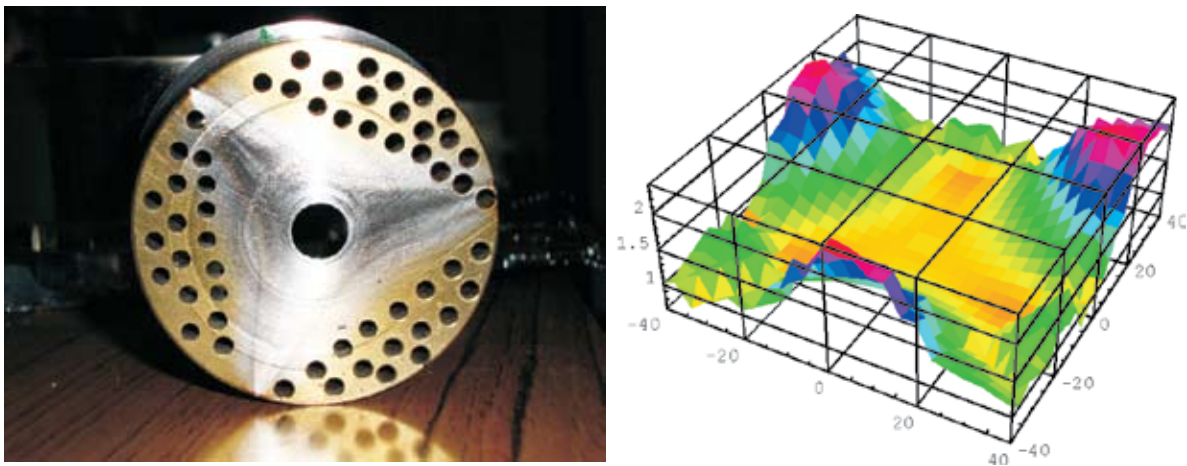


Fig. 2. View of the plasma electrode at $z = 98$ mm ; simulated model of the loss triangle at position 98 mm from the source centre ; (dimensions in mm, magnetic field values in Tesla)

D. Emittance measurements of multiply charged ions from PKDELIS ECR ion source

For the High Current Injector project at Inter University Accelerator Centre (IUAC), the HTS ECR ion source, PKDELIS will deliver high charge state ions. The emittance of the ECR ion source is an important parameter to design further beam transport system and to match the acceptances of the downstream Radio Frequency Quadrupole and Drift Tube Linac accelerators of the High Current Injector [7]. Emittance measurements have been performed utilising the ‘three beam size’ technique. A slit and two BPM’s kept at fixed distances apart has been used to measure the beam size. The digitized beam profiles has been analysed to extract the emittance of various multiply charged ions. The emittance values measured for oxygen, argon and xenon beams are shown in figure 3 at an extraction voltage of 15.15 kV using a slit width of 5 mm.

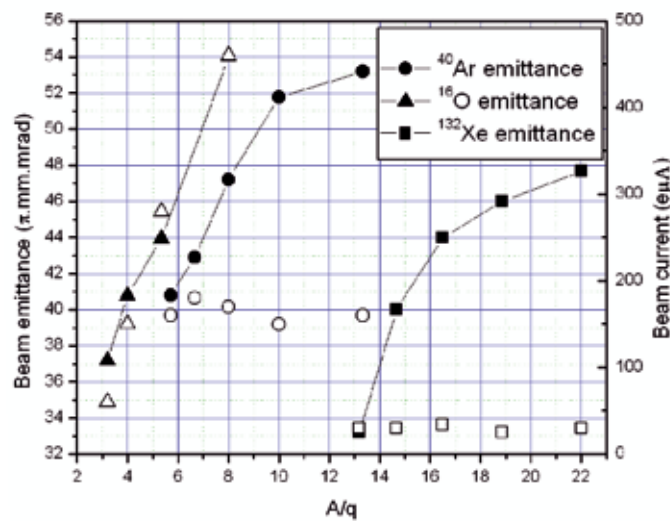


Fig 3. Measured emittance values for O₂, Ar and Xe at an extraction voltage of 15.15 kV using a slit width of 5mm

E. Status of development of 2.45 GHz high current proton ECR ion source

As a part of ion source development programme, a permanent magnet 2.45GHz ECR ion source has been planned to be developed indigenously at IUAC. The main aim is to reduce the cost and at the same time to get the best performance from such a source. A permanent magnet structure for the 2.45 GHz ECR ion source which is capable of producing high intensity low charge state ion beams has been designed and fabricated. NdFeB magnets are used and arranged in the form of two coaxial rings having 6 segments in each ring, around the plasma chamber. A stainless steel, magnet pole holder has been designed for assembling the magnet segments in such a way that each pole can be locked

separately after mounting the magnet segment inside the pole holder. Field mapping of the fabricated structure has been completed for both the rings and shown in figure 4. The simulations of the rf coupling to the source using a matching transformer is underway. This will concentrate the electric field close to the axis of the source to improve the coupling. In order to save costs for this development project especially for the RF power source, commercial available microwave ovens which have been utilized instead. These are being converted so that the rf power is coupled to the load in CW mode. The plasma chamber is presently under design considerations and fabrication is expected to start soon. A tentative, multi-electrode extraction system has been designed to facilitate extraction of intense proton beams.

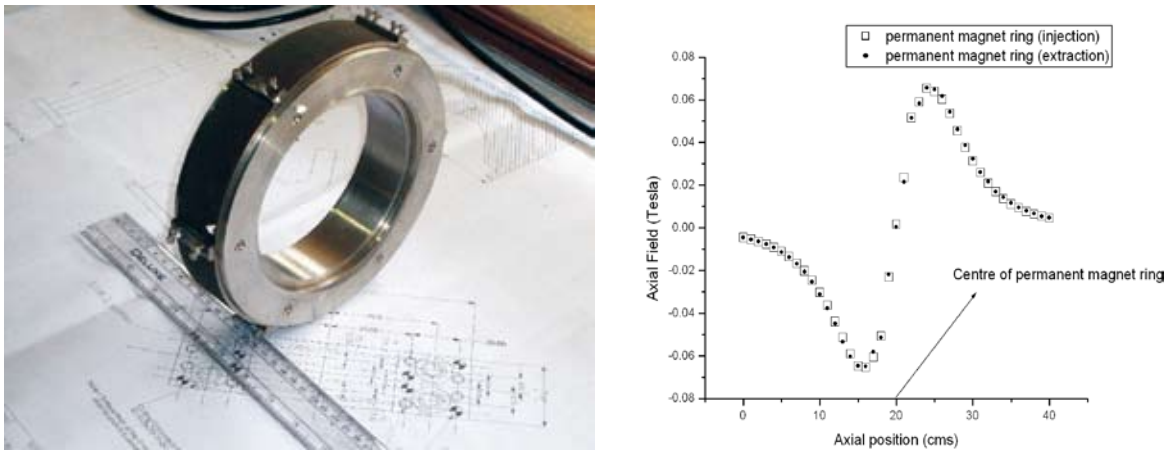


Fig. 4. Fabricated view of one of the magnetic rings (left) and measured field (right)

REFERENCES

- [1] C. Bieth, S. Kantas , P. Sortais , D. Kanjilal , G. Rodrigues , S. Milward, S. Harrison , R. Mc Mahon, Nucl.Instrum.Meth., B 235 (2005)498.
- [2] D.Kanjilal, G.Rodrigues, P.Kumar, A.Mandal, A.Roy, C.Bieth, S.Kantas, P.Sortais, Review of Scientific Instruments,77,03A317 (2006).
- [3] A. Mandal,, G. Rodrigues, D. Kanjilal, Peter Brodt, Franz Bødker, Nuclear Instruments and Methods in Physics Research A 583 (2007) 219–227.
- [4] R.Baskaran, T.S.Selvakumaran, G.Rodrigues, D.Kanjilal, A.Roy, Review of Scientific Instruments,79, 2008.
- [5] A.Mandal, G.Rodrigues, D.Kanjilal, A.Roy, Physics Procedia 1 (2008)105, Proceedings of the Seventh International Conference on Charged Particle Optics.
- [6] G.Rodrigues, P.S.Lakshmy, R.Baskaran, D.Kanjilal, A.Roy, Rev.Sci.Instrum.Vol 81,02A323 (2010).
- [7] G.Rodrigues, P.S.Lakshmy, Sarvesh Kumar, A.Mandal, D.Kanjilal, R.Baskaran, A.Roy, Rev.Sci. Instrum. Vol 81,02B713 (2010).
- [8] G.Rodrigues, P.S.Lakshmy, P.Kumar, A.Mandal, D.Kanjilal & A.Roy, Indian Journal of Cryogenics, Vol.34, No.1-4,2009, pg113.

2.6 HIGH POWER RF TEST ON THE 1.17M MODULATED PROTOTYPE RFQ ACCELARTOR

C.P. Safvan, Sugam Kumar, R. Ahuja, R. Mehta, A. Kothari, R.V. Hariwal, D. Kanjilal, A. Roy

This year low power and high power RF test has been done on modulated prototype RFQ. Base plate and the cavity chamber were copper plated to improve the quality factor. Power coupler made of copper tube of diameter 6mm and length 500mm was used to couple power into the cavity. Loop size was optimized to get the coupling coefficient nearly equal to one which is the condition for maximum power transfer to the cavity and minimum reflection; this is also called critical coupling condition. The optimized coupling coefficient measured was 0.84. The resonance frequency and loaded quality factor were measured with a Network Analyzer. Measured values are 53.02MHz and 1692 respectively and the calculated intrinsic quality factor is 3112, while ideal (simulated) values are 48.5MHz and 4000. Shunt impedance is found to be 79.8 k-ohm as compare to 80 k-ohm, which is, designed value of unmodulated part. Power required to generate 70kV Intervane voltage is coming out to be 30.69kW.

For high power RF tests, a 35kW commercial RF amplifier has been purchased. Cooling channels have been made adequately to cool the vanes and post during high power RF power feed. The maximum power fed into the RFQ was 10kW. Power coupler was cooled through normal water and there was no abnormal heating observed in the coupler. The cooling to the vanes and vanes supports were found to be satisfactory. At 10kW of input power the temperature of the water was found to be increased by 2 degree. Since chamber is not equipped with cooling channels there were local heating observed at different locations on the base plate. Because of heating of chamber the resonance frequency was shifting continuously with increasing the input power. This was offset by changing the frequency of the driver amplifier.

2.6.1 Development of Drift Tube Linac at IUAC

B.P. Ajithkumar, J. Zacharias, R. Mehta, Sugam Kumar, R.V. Hariwal

The High Current Injector (HCI) project at Inter University Accelerator Centre uses a Radio Frequency Quadrupole (RFQ) and Drift Tube Linac (DTL) combination to accelerate heavy ions, $A/q \leq 6$, from an ECR ion source to inject them to the existing superconducting LINAC. Layout of the HCI project is shown in annexure 1. The DTL has been designed to accelerate ions from 180 keV/u to 1.8 MeV/u, using six IH type RF resonators operating at 97 MHz. The required output energy of the DTL is decided by the minimum input velocity of nearly 6% of velocity of light, required for the existing superconducting LINAC. IH type resonators are the preferred choice for multiple gap DTL applications due to their high shunt impedance values. The frequency of operation is chosen as 97 MHz after comparing with the

48.5 MHz option. The later offers a larger acceptance but the size of the resonator becomes much larger at this frequency. The beam dynamics and generation of the drift tube geometry is done using the LANA code.

A simplified schematic block diagram of the accelerating structure is shown below. The table shows the length, number of cells and the energy gain of each resonator.

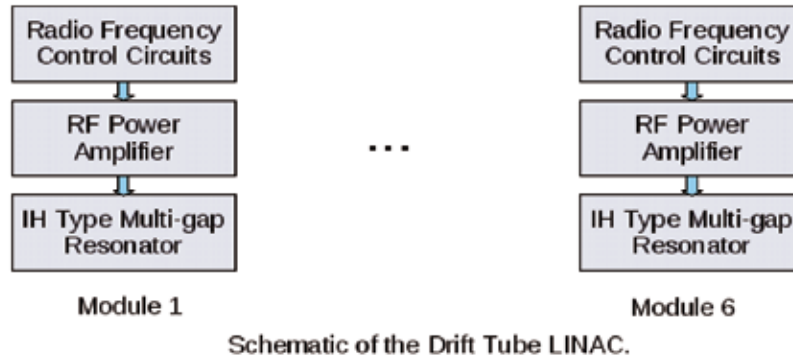


Table 1: Length, number of cells and output energy for the six cavities.

Length (cm)	Number of Cells	Output Energy (MeV/u)
38.5	11	0.32
73.4	13	0.55
94.4	13	0.85
86.5	11	1.15
92.2	11	1.46
81.6	9	1.8

Beam Dynamics

Each IH tank is independently phased from separate RF amplifiers. With the exception of the first and last tank the tanks consist of bunching sections and accelerating sections. The accelerating sections in the IH tanks are designed for 0° synchronous phase. The beam is injected into the accelerating sections with a reduced phase spread and velocity higher than the design velocity so that the bunch drifts to more negative phases during acceleration and emerges with a reduced energy spread. Quadrupole triplets between tanks provide periodic transverse focusing. Short -60° sections at the entrance of every accelerating tank provide periodic longitudinal focusing to allow matching to the next accelerating section. Key to achieving an improved longitudinal acceptance is the addition of an extra long drift-tube between the bunching and accelerating sections to further reduce the phase spread entering the accelerating section. With this novel technique a beam of more than 3 keV/u-nsec can be accelerated with minimal emittance growth.

The velocity of the incoming beam (2% of c) and the chosen resonant frequency (97 MHz) results in a gap length of about 1.5 cm for the first resonator. The inner diameter of the tube is fixed at 1.4 cm to minimize the penetration of field into the tubes. The length of the tanks are chosen in such a way that for the given input emittance ($\epsilon = .3 \text{ mm mrad}$ normalized), the maximum beam size inside any drift tube is less than half of the tube inner radius. The transverse beam envelope is shown in Figure 1. After each resonator, a magnetic quadrupole triplet is used for focusing the beam in the transverse direction.

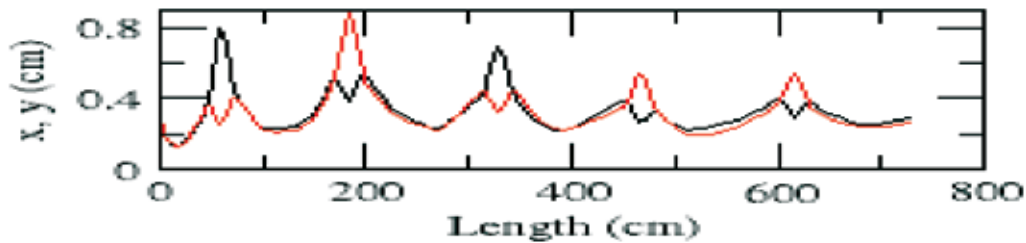


Fig. 1. Transverse beam envelopes for a normalized input emittance of 0.3 pi mmmr .

Design Considerations

The beam tubes and their supporting structures will be made from Oxygen Free Copper. The body of the cylindrical resonator for the first prototype was made of stainless steel 304 (SS-304). Inner surface of the housing will be copper plated. Due to problem faced in copper plating of prototype radio frequency quadrupole, we are exploring the options of using solid copper for the DTL resonator body.

Multi gap DTL structures can be of Alvarez type or Interdigital H type. Out of these options IUAC decided to opt for inter-digital H type (IH) structure. IH type structure offers high shunt impedance due to reduced drift tube capacitance [1].

Prototype Development

In order to validate the design, a full scale prototype IH type resonator was made. The cavity was designed in CST Microwave studio. The prototype is fabricated using SS304 material. Flanges and all ports are welded in and the vacuum test was carried out successfully. The cavity has an inner diameter of 85 cm and length of 38 cm after final fabrication. The ridges which hold the stems of the drift tubes are made from aluminium, and the stems and drift tubes are made from copper as well as aluminium. The 11 gap IH structure has 10 drift tubes, each supported alternately from top and bottom. The machining of the ridges, stems and drift tubes has been done using the in-house CNC vertical milling machine. Provision for water cooling has been made in each of the stems as well as the end walls of the cavity.

Low power RF tests were conducted on the prototype cavity. For determining the various parameters, bead pull tests and network analyzer based measurements were carried out. The measured resonant frequency of the prototype was near 98 MHz and it was brought to the design value of 97 MHz by using a tuner plate on one side. A bead pull test was done to measure the electric field profile along the beam axis. A sapphire bead was pulled along the beam axis of the cavity and the resonant frequency measured. The shift of the resonant frequency caused by the presence of the bead is proportional to the electric field at the position of the bead. It can be seen that even though the uniformity of the electric fields in the central gaps has been achieved to a large extent, the end gaps have a smaller field than expected. This discrepancy can be explained by the end gaps that were larger than specified due to manufacturing issues, and will be corrected in the final tank.

Present Status

The prototype of the first resonator cavity is being tested at low power. The resonant frequency and electric field profile along the beam axis is in agreement with the calculations. Attempts were made to do copper plating on stainless steel but the results are not fully satisfactory. Copper has been ordered to make a prototype with solid copper body. A 10 kW RF power amplifier has been procured and tested. Once the prototype is complete a full power test will be done.